Geophysical Research Letters

Key Points:
- Double charge exchange of protons produces negative H ions in the solar wind
- The measurements agree with published laboratory cross sections and energy deficits
- The cross sections and energy deficits are estimated for the first time in the space environment

Correspondence to:
J. L. Burch,
jburch@swri.edu

Charge exchange in cometary coma: Discovery of H⁻ ions in the solar wind close to comet 67P/Churyumov-Gerasimenko

J. L. Burch[1], T. E. Cravens[2], K. Llera[3], R. Goldstein[1], P. Mokashi[1], C.-Y. Tzou[4], and T. Broiles[1]

[1]Southwest Research Institute, San Antonio, Texas, USA, [2]Physics and Astronomy Department, University of Kansas, Lawrence, Kansas, USA, [3]Physics and Astronomy Department, University of Texas at San Antonio, San Antonio, Texas, USA, [4]Physics Institute, University of Bern, Bern, Switzerland

Abstract As Rosetta was orbiting comet 67P/Churyumov-Gerasimenko, the Ion and Electron Sensor detected negative particles with angular distributions like those of the concurrently measured solar wind protons but with fluxes of only about 10% of the proton fluxes and energies of about 90% of the proton energies. Using well-known cross sections and energy-loss data, it is determined that the fluxes and energies of the negative particles are consistent with the production of H⁻ ions in the solar wind by double charge exchange with molecules in the coma.

1. Introduction

Investigation of the solar wind interaction with comets is an important objective of the European Space Agency (ESA) Rosetta mission. This investigation is conducted by the Rosetta Plasma Consortium [*Carr et al.*, 2007], which includes the Ion and Electron Sensor (IES) [*Burch et al.*, 2007] among other instruments measuring magnetic fields [*Glassmeier et al.*, 2007], plasma densities and temperatures [*Eriksson et al.*, 2007], ion composition [*Nilsson et al.*, 2007], and plasma waves [*Trotignon et al.*, 2007] on the Rosetta Orbiter. The instruments are controlled by a Plasma Interface Unit, which acquires and transmits their data to the spacecraft.

Expectations for the interaction of the solar wind with comet 67P were based on theoretical models and previous measurements from flyby missions [*Mendis*, 1988]. As Rosetta approached the comet, the expected buildup of plasma densities, pickup of cometary ions into the solar wind [*Nilsson et al.*, 2015; *Goldstein et al.*, 2015], charge exchange of solar wind He^{++} producing He$^+$ ions [*Shelley et al.*, 1987; *Chaizy et al.*, 1991], and charged dust or ice grains were observed by IES. In this paper, we report an unpredicted and, to our knowledge, not previously observed phenomenon—energetic negative particles in the solar wind. We show evidence that these particles are negative hydrogen ions produced by double charge exchange of solar wind protons with the neutral gas of the coma, the densities of which were measured concurrently by the Rosetta Orbiter spectrometer for ion and neutral analysis (ROSINA) instrument [*Balsiger et al.*, 2007]. The energies and angular distributions of these particles are very similar to those of the solar wind protons, their fluxes are about 10% of the proton fluxes, and their energies are about 90% of the proton energies. These percentages are shown to be consistent with well-known charge exchange cross sections and with theoretical and experimental values of energy loss for double charge exchange of H$^+$ for the measured neutral gas densities.

2. Instrumentation and Data

IES measures ions and electrons with energy/charge from 4 eV to 18 keV with 8% energy resolution and 5°×22.5° angular resolution for electrons and 5°×45° for ions, with the ion sector normally containing the solar wind segmented into nine 5°×5° channels. Because of the low data rates available (~265 b/s in burst mode), averaging over adjacent energy and/or angular channels is typically necessary. Because Rosetta is a three-axis stabilized spacecraft with no scan platform, IES performs electrostatic scanning of its intrinsic 5°×360° azimuthal field of view (FOV) over ±45° yielding sixteen 5° elevation angle channels and a total FOV of 2.8π steradians. IES is mounted on a corner of the spacecraft with the symmetry axis of the toroidal tophat analyzers centered on a 45° angle from the local spacecraft zenith in order to maximize viewing of both the solar wind and the comet for most anticipated spacecraft orientations. While this objective is generally achieved, there are

Oct. 17, 2014 (Day 290)
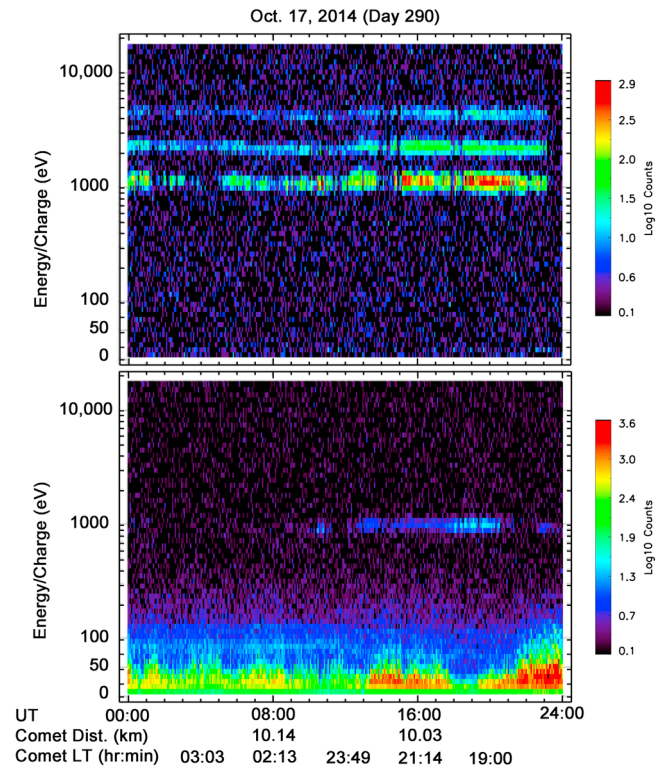
Figure 1. Energy-time spectrogram of (top) ion and (bottom) electron count rates on 17 October 2014 when both sensors viewed in the direction toward the Sun. Note the different color scales for ions and electrons.

unavoidable obstructions for some azimuths at certain elevation angles that graze the spacecraft. These obstructions are kept in mind and avoided during data analysis.

During the time period of the observations reported here (mid-September to mid-November 2014), Rosetta was orbiting close to the comet (10–30 km) in terminator orbits at heliocentric distances of 3.4 AU (in September) to 3.0 AU (in November). Ion and electron energy-time spectrograms are shown in Figure 1 from the azimuths and elevation angles of IES that were pointed directly at the Sun on 17 October 2014.

Clearly seen in the ion spectrogram (Figure 1, top) are the solar wind ions (protons in the bottom trace and He^{++} in the middle trace). The upper trace is identified as He^{+}, which is produced by charge exchange of solar wind He^{++} as first detected at comet Halley by *Shelley et al.* [1987]. Figure 1 (bottom) is the electron energy-time spectrogram. In addition to the low-energy electrons, which are an admixture of

solar wind electrons and cometary coma electrons, there is a clear trace near 1 keV with energy spectra that are similar to those of the solar wind ions.

Polar spectrograms for ions and electrons averaged over the time period 18:00 to 20:30 UT on 17 October 2014 are shown in Figure 2. The polar spectrograms are two-dimensional angular distributions showing fluxes for all azimuths at the elevation angle ranges for negative and positive particles, respectively, which contain the solar wind direction. In the particular mode that was used on this day, the azimuth angle resolution was 45°, and except for the case of the protons in Figure 2a, counts were registered in only one anode (azimuth bin) at the solar wind energies. The fact that all of the positive and negative particles at these energies are highly collimated in the solar wind direction supports the identification of the negative particles as H^{-} ions. We note also in Figure 2a a peak at about 15 eV, which is caused by a negative spacecraft potential, accelerating local thermal ions into the instrument. Although no significant ion pickup was observed on 17 October 2014, later in the time period studied (by November 2014) significant ion pickup was observed as described for Halley's comet by *Neugebauer et al.* [1987] and for Rosetta by *Goldstein et al.* [2015].

Figure 3 shows average energy spectra of the positive and negative particles observed between 18 and 21 UT on 17 October 2014. In the operating mode used on that day, two adjacent energy channels (out of the 124 channels) were averaged together. The average sampled energy at the peak of the proton spectrum was 1079 eV while that at the peak of the negative particle spectrum was 973 eV—a difference of 106 eV. As noted later, part of this energy difference is caused by the spacecraft potential of about −15 V, which was pointed out in connection with Figure 2a. The flux within the proton and negative particle peaks can be calculated by summing the differential flux in the five energy bands surrounding each peak:

$$\sum_{E_1}^{E_5} J(E_i)\triangle E_i = 5.80 \times 10^7 \, \text{cm}^{-2}\text{s}^{-1} \quad \text{for negative particles and}$$

$$(1)$$

$$\sum_{E_1}^{E_5} J(E_i)\triangle E_i = 5.64 \times 10^8 \, \text{cm}^{-2}\text{s}^{-1} \quad \text{for H}^{+}$$
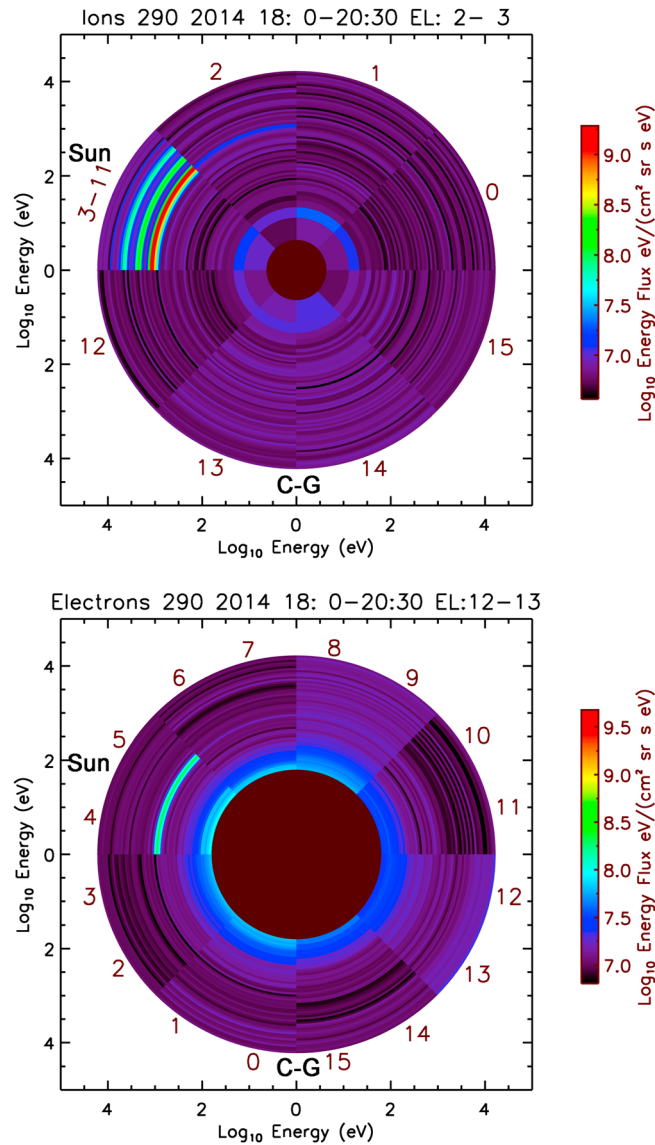
Figure 2. (a) Polar spectrogram of energy flux versus energy in the plane containing the solar direction (elevation angles 2 and 3). Anode numbers are listed around the plot. In the mode used at this time anodes 3–11, which each have 5° viewing angles are added together on board to accommodate the low downlink rate. Within anodes 3–11 are seen H^+, He^{++}, and He^+ ions along with possibly another ion at higher energies. The viewing directions toward the Sun and comet C-G are noted. (b) Same as Figure 2a except for negative particles. Low-energy electrons (<50 eV are blocked out). The anode numbers are different from those of the positive ions with anodes 4–5 viewing the Sun in this case. A negative beam with energy slightly less than the proton energy is clearly seen in anodes 4–5.

The ratio of the negative particle fluxes to the H^+ fluxes is 0.103. This value is compared to the results of charge exchange calculations in section 3.

Figure 4 is a line plot of proton fluxes (top), negative particles (middle), and neutral gas density (bottom) for the time period 14 to 22 UT on 17 October 2014. The particle fluxes are highly variable, while the neutral gas density has a single well-defined peak. We note that while there are two major regions of high proton fluxes (~15–16 UT and 19–21 UT), there is only one peak in the negative particle fluxes, and this peak lines up approximately with the peak in neutral gas density. Returning to Figure 1, we note that the peaks in negative particle flux and neutral gas density lie between the regions of high fluxes of low-energy electrons (solar wind electrons and/or coma photoelectrons).

The major features in the data shown in Figures 1–4 are the following:

1. The positive ion spectrogram in Figure 1 shows solar wind protons, alpha particles, and He^+ ions (from charge exchange of alpha particles within the coma neutral gas (as observed and interpreted previously by *Shelley et al.* [1987])).

2. The negative particle spectrogram in Figure 1 shows a beam at, but slightly below, the proton energy with energy fluxes of a few percent of that of the protons. These differences in energy are shown more clearly in the energy spectra of the positive ions and negative particles (Figure 3). The negative particle spectrogram also shows that the strongest negative particle beam occurs between two regions of enhanced low-energy electron fluxes.

3. Polar spectrograms in Figure 2 show that both the protons and the negative particle beams are contained almost completely within the angular sector containing the Sun.

4. Energy spectra for the positive and negative particles in Figure 3 show a negative particle peak at an energy of about 90% of that of the H^+ energy peak and a negative particle flux of about 5.1% of the H^+ flux. Also shown in Figure 3 are energy peaks for He^{++} and He^+, which had been determined before by Giotto to result from charge exchange of He^{++} with the coma neutral gas.
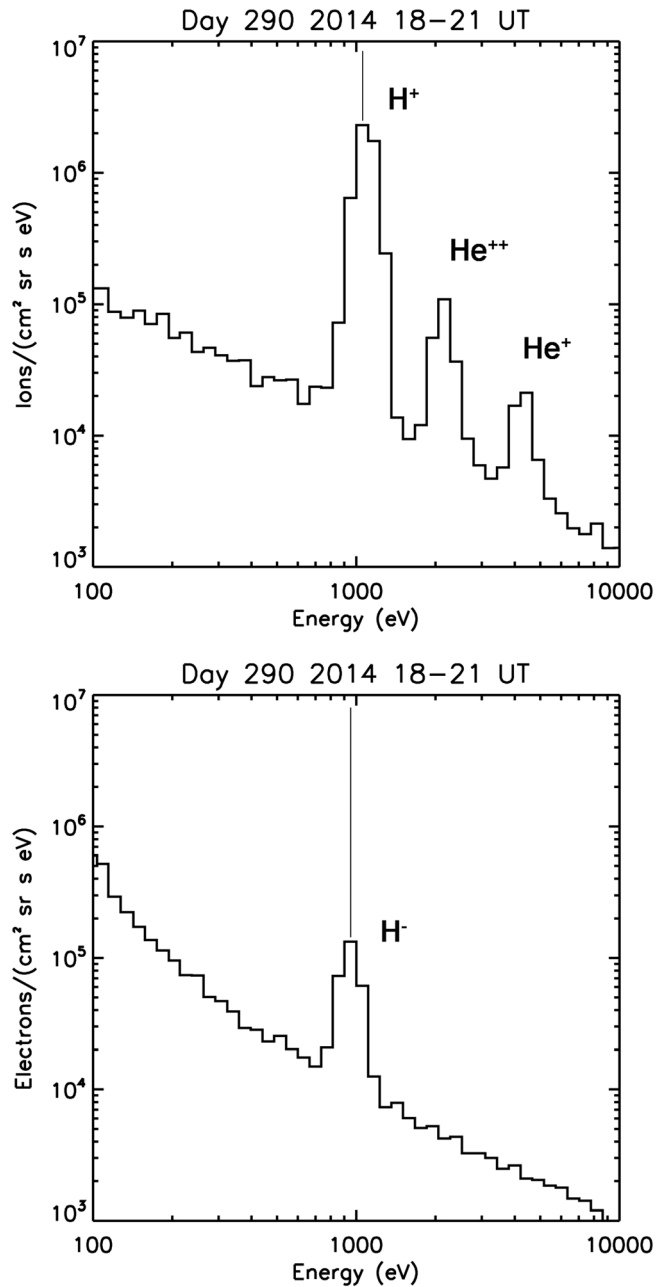
Figure 3. Energy spectra for (top) positive ions and (bottom) negative particles. At increasing energies, the positive ion spectrum includes H^+, He^{++}, and He^+, while the negative particle spectrum shows a single peak with a peak flux of about 5% of the proton flux, a total flux of about 10% of the proton flux, and a peak energy of about 90% of the proton energy peak (as noted in Figure 1).

5. Line plots of proton and negative particle counts compared to measured neutral gas densities in Figure 4 show that the negative particle counts peak in the same general region as the peak in neutral gas density.
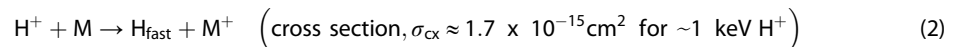
These observations led us to propose the hypothesis that double charge exchange of the solar wind proton beam within the coma neutral gas is the source of the negative particles, which are H^- ions. An alternative explanation involving attachment of low-energy electrons to solar wind ions is not considered because of the anticorrelation shown in Figure 1 between the negative particle beam and the low-energy solar wind and/or coma electrons. In the next section our hypothesis is tested by a charge exchange analysis.
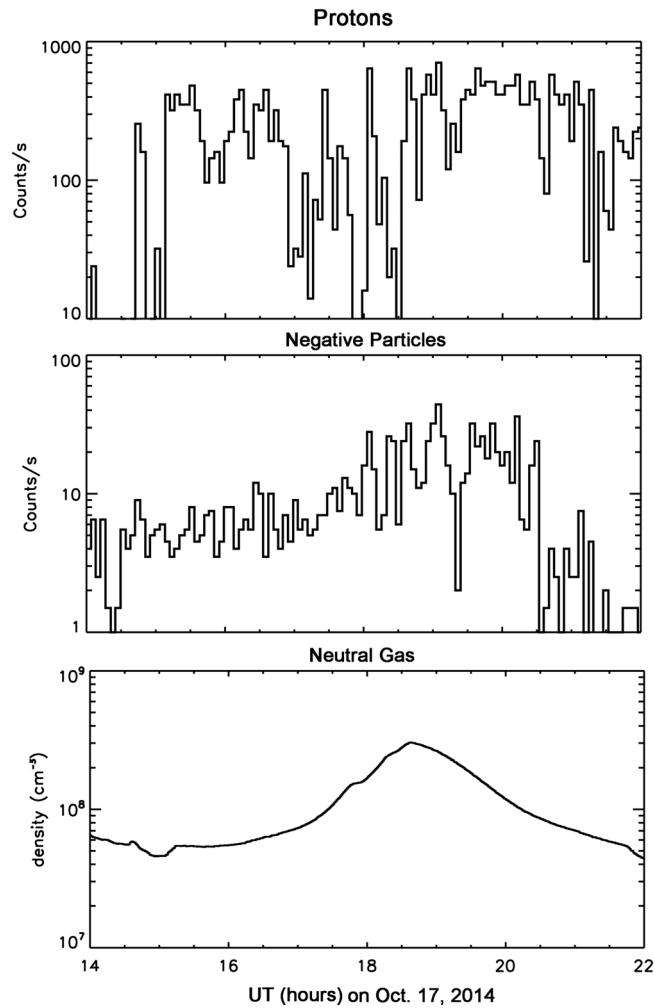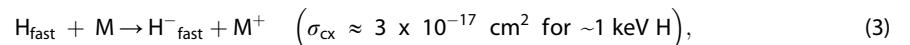
Figure 4. Count rates for (top) protons and (middle) negative particles both at the peak beam energies shown in Figure 3. (bottom) Neutral gas density measured by the ROSINA COPS sensor.

3. Charge Exchange Analysis

Charge exchange reactions of solar wind H^+ with molecules in the cometary coma can be expressed in a general sense as

$$H^+ + M \rightarrow H_{fast} + M^+ \quad \left(\text{cross section, } \sigma_{cx} \approx 1.7 \times 10^{-15} cm^2 \text{ for } \sim 1 \text{ keV } H^+ \right) \quad (2)$$

where M is the neutral target (H_2O, CO_2, OH, etc.). This reaction results in a fast neutral hydrogen atom and a cold charged molecule. Cross sections for this reaction are fairly well known (e.g., *Lindsay et al.* [1997], for H_2O). A subsequent reaction leading to electron attachment to the fast neutral H beam can be expressed as

$$H_{fast} + M \rightarrow H^-_{fast} + M^+ \quad \left(\sigma_{cx} \approx 3 \times 10^{-17} cm^2 \text{ for } \sim 1 \text{ keV } H \right), \quad (3)$$

resulting in a fast negative hydrogen atom and a positively charged cold molecule. Cross sections for such reactions are also fairly well known [e.g., *Fedorenko*, 1970; *Dimov and Dudnikov*, 1978]. The neutral density in the coma is measured by the cometary pressure sensor (COPS) sensor of ROSINA [*Balsiger et al.*, 2007], and these measured densities are used in our calculations of negative ion flux to compare with the IES data.

The flux of H from solar wind H^+ is the integral over the path/streamline (assumed to be radial) of the H production rate, $P = n_n(r) \sigma_{cx} F_{sw}(r)$, where $n_n(r)$ is the neutral density and $F_{sw}(r)$ is the solar wind flux. In order to estimate $n_n(r)$, we express the neutral density for a single species as a function of radius as

$n_n(r) = [Q/(4\pi u_n r^2)]\exp(-r/\lambda)$, where Q is the production rate, u_n is the outflow velocity, and λ is the neutral attenuation length due to ionization [*Haser*, 1957; *Cravens*, 1991]. Since λ is $\gg 10^6$ km at the comet solar distance of ~3.5 AU [*Cravens*, 1991], we set λ equal to infinity for this estimate so that $n_n(r) = [Q/(4\pi u_n r^2)]$. F_{sw} is approximately independent of r, and the H flux can be estimated as $F_H(r) \approx N_n(r) \sigma_{cx} F_{sw}$, where $N_n(r)$ is the integrated column density of neutrals from the cometocentric distance r of the observation out to infinity:

$$N_n(r) = \int_r^\infty n_n(r)\mathrm{d}r = rn_n(r) \tag{4}$$

Note that $N_n(r) \sigma_{cx} \approx 0.1$, so the approximation of unattenuated proton flux is good to about 10%.

As noted above, a second charge exchange reaction can convert a fraction of the H beam to H^-. The production rate for this reaction is $P^-(r) = n_n(r) \sigma_- F_H(r)$, and the H^- flux is given by the integral of $P^-(r)$ from r_o (the observation point) out to infinity.

The negative hydrogen flux is then,

$$F_{H^-} = F_{SW}\sigma_{cx}\sigma_- \int_{r_o}^\infty N_n(r)n_n(r)\mathrm{d}r = 0.5F_{SW}\sigma_{cx}\sigma_- r_o^2 n_n^2(r_o). \tag{5}$$

With $r_o \approx 10$ km and $n_n(r_o) \approx 2 \times 10^8$ cm^{-3} (Figure 4), $F_{H^-} \approx 5.1 \times 10^{-2} F_{sw}$. This ratio is consistent with the energy spectra observations shown in Figure 3, which were shown to indicate this same peak flux ratio and a total flux ratio within a factor of 2 ($F_{H^-} \approx 1.03 \times 10^{-1} F_{sw}$).

Experimental data are also available on the cross sections for double charge exchange (σ_{dcx}) [*Ali*, 1969; *Fedorenko*, 1970], and this value is approximately 1.5×10^{-18} cm^2 at proton energies near 1 keV interacting with Argon or O_2:

$$\begin{aligned} H^+ + M &\to H^- + M^{++} \quad \text{or} \\ H^+ + M &\to H^- + M_1^+ + M_2^+. \end{aligned} \tag{6}$$

The flux of H^- resulting from this reaction will be given by

$$F_{H^-} \approx r_o n(r_o) \sigma_{dcx} F_{sw} = 3 \times 10^{-3} F_{sw}. \tag{7}$$

Thus, the two-step process should be more important for producing H^- ions in the solar wind.

All of these reactions have an energy deficit, which is caused by a combination of excitation, ionization, and the energy required for the transfer of the electron from the parent molecule to the receiving beam particle. Calculated and measured values are in the range of 33–36 eV depending on the species and on whether or not the ionized molecule is dissociated [*Dalgarno and Griffing*, 1958; *Hurley and Maslen*, 1961; *Dorman and Morrison*, 1963]. For example, the mean specific energy per ion pair is 33 eV for a proton beam in O_2 gas [*Dalgarno*, 1962]. This energy deficit is most likely responsible for the lower energies of the negative ions with respect to the solar wind protons, as shown in the next section. For the two-step process the energy deficit would occur twice so that the H^- beam energy would be expected to be about 66–72 eV less than the proton energy. Recall in Figure 2a that we noted a peak at ~15 eV in all directions, which are locally produced cometary ions that have been postaccelerated by a negative spacecraft potential (~ −15 V) [*Goldstein et al.*, 2015]. The negative spacecraft potential decelerates the H^- and accelerates the protons each by ~15 eV, resulting in a ~30 eV total energy difference between the two species. As shown in Figure 3, the energy deficit is shown by our observations to be about 106 eV. If 30 eV is caused by the spacecraft potential, then the energy deficit from charge exchange amounts to 76 eV, which compares favorably to the 66–72 eV prediction from theory and lab measurement. The difference is within the error caused by adjacent IES energy bands being averaged together with the resulting energy sample widths being 97 eV and 107 eV for negative particles and H^+, respectively.

4. Summary and Conclusions

When orbiting very close to comet C-G (~10 km) the IES instrument on Rosetta observed the solar wind with an embedded negative particle beam in the solar wind direction with energy of about 90% of the solar wind

proton energy. The flux of the negative particles was observed to be approximately 10% of the solar wind proton flux. We tested the hypothesis that the negative particles are H^- ions produced by double charge exchange of solar wind protons with the molecules of the cometary coma. Using the available charge exchange cross sections, simultaneous measurements of the neutral gas density, and theoretical and experimental values of the charge exchange energy loss, both the flux and energy ratios between the hypothesized H^- beam and the proton beam were closely matched within reasonable experimental uncertainties. Since the negative particle fluxes were anticorrelated with the observed low-energy electron fluxes, an alternative hypothesis involving electron attachment was rejected.

We believe these observations of H^- ions embedded in the solar wind to be the first of their kind. Negative ions were observed by Giotto upstream of comet Halley [*Chaizy et al.*, 1991], but these observations were of thermal coma ions, which appeared at higher energies because of the rapid motion of Giotto with respect to the comet. Rosetta, on the other hand, has a very low velocity (a few m/s) relative to the comet and so is in a unique position to measure in situ phenomena such as charge exchange, which are important aspects of the solar wind comet interaction.

Since the initial observation of negative hydrogen ions in the solar wind, they have continued to be observed by IES close to the comet on most days through January 2015 as the spacecraft orbited within altitudes of ~30 km while the distance of the comet from the Sun was decreasing to ~2.5 AU.

Finally, it is reasonable to consider any coma ion chemistry effects that may result from the observed H^- ions. Existing coma chemistry models focus on the dense inner comas of active comets where the plasma is rather cold, while the H^- in the current study is quite energetic (i.e., ~1 keV) and, once formed, is not confined to the inner coma. Therefore, we expect the implications of the observed H^- ions for existing cometary chemistry models to be minor.

References

Ali, D. E. (1969), Measurements of negative ion production in atmospheric gases, NASA Contractor Report CR-1406, Ames Research Center.

Balsiger, H., et al. (2007), ROSINA–Rosetta Orbiter spectrometer for ion and neutral analysis, *Space Sci. Rev.*, *128*, 745–801, doi:10.1007/s11214-006-8335-3.

Burch, J. L., R. Goldstein, T. E. Cravens, W. C. Gibson, R. N. Lundin, C. J. Pollock, J. D. Winningham, and D. T. Young (2007), RCP-IES: The ion and electron sensor of the Rosetta Plasma Consortium, *Space Sci. Rev.*, 697–712, doi:10.1007/s11214-006-9002-4.

Carr, C., et al. (2007), RPC: The Rosetta Plasma Consortium, *Space Sci. Rev.*, *128*, 629–647, doi:10.1007/s11214-006-9136-4.

Chaizy, P., et al. (1991), Detection of negative ions in the coma of comet P/Halley, *Nature*, *349*, 393–396.

Cravens, T. E. (1991), Plasma processes in the inner coma, in *Comets in the Post-Halley Era*, vol. 2, edited by R. L. Newburn Jr. et al., pp. 1211–1255, Kluwer Acad. Pub., Netherlands.

Dalgarno, A. (1962), Range and energy loss, in *Atomic and Molecular Processes*, edited by D. R. Bates, pp. 622–642, Academic Press, New York.

Dalgarno, A., and G. W. Griffing (1958), Energy per ion pair for electron and proton beams in atomic Hydrogen, *Proc. R. Soc. London, Ser. A*, *248*, 415–428.

Dimov, G. I., and V. G. Dudnikov (1978), Control of particle flow by charge exchange, *Fusion Phys.*, *4*, 692.

Dorman, F. H., and J. D. Morrison (1963), Ionization potentials of doubly charged oxygen and nitrogen, *J. Chem. Phys.*, *39*, 1906, doi:10.1063/1.1734559.

Eriksson, A. I., et al. (2007), RPC-LAP: The Rosetta Langmuir probe instrument, *Space Sci. Rev.*, *128*, 729–744, doi:10.1007/s11214-006-9003-3.

Fedorenko, N. V. (1970), Electron loss and capture by hydrogen atoms, protons, and negative ions in the collision with atoms and molecules —Experimental data on cross sections, *Zh. Tekh. Fiz.*, *40*, 2481–2497.

Glassmeier, K.-H., et al. (2007), RPC-MAG: The fluxgate magnetometer in the Rosetta Plasma Consortium, *Space Sci. Rev.*, *128*, 649–670, doi:10.1007/s11214-006-9114-x.

Goldstein, R., et al. (2015), The Rosetta Ion and Electron Sensor (IES) measurement of the development of pickup ions from Comet 67P/Churyumov-Gerasimenko, *Geophys. Res. Lett.*, *42*, 3093–3099, doi:10.1002/2015GL063939.

Haser, L. (1957), Distribution d'intensité dans la tête d'une comète, *Bull. Cl. Sci., Acad. R. Belg.*, *43*, 740–750.

Hurley, A. C., and V. W. Maslen (1961), Potential curves for doubly positive diatomic ions, *J. Chem. Phys.*, *34*, 1919, doi:10.1063/1.1731793.

Lindsay, B. G., D. R. Sieglaff, K. A. Smith, and R. F. Stebbings (1997), Charge transfer of 0.5-, 1.5-, and 5-keV proton with H_2O: Absolute differential and integral cross sections, *Phys. Rev.*, *A55*, 3945–3946.

Mendis, D. A. (1988), A postencounter view of comets, *Ann. Rev. Astron. Astrophys.*, *26*, 11–49, doi:10.1146/annurev.aa.26.090188.000303.

Neugebauer, M., et al. (1987), The pick-up of cometary protons by the solar wind, *Astron. Astrophys.*, *187*, 21–24.

Nilsson, H., et al. (2007), RPC-ICA: The ion composition analyzer of the Rosetta Plasma Consortium, *Space Sci. Rev.*, *128*, 671–695, doi:10.1007/s11214-006-9031-z.

Nilsson, H., et al. (2015), Birth of a comet magnetosphere: A spring of water ions, *Science*, *347*, doi:10.1126/science.aaa0571.

Shelley, E. G., S. A. Fuselier, H. Balsiger, J. F. Drake, J. Geiss, B. E. Goldstein, R. Goldstein, W. H. Ip, A. J. Lazarus, and M. Neugebauer (1987), Charge exchange of solar wind ions in the coma of comet P/Halley, *Astron. Astrophys.*, *187*, 304–306.

Trotignon, J. G., et al. (2007), RPC-MIP: The mutual impedance probe of the Rosetta Plasma Consortium, *Space Sci. Rev.*, *128*, 713–728, doi:10.1007/s11214-006-9005-1.